ELSEVIER

0144-8617(95)00034-8

Carbohydrate Polymers **27** (1995) 47–52

0144-8617/95/$09.50+.00

Crystallization of amylose–fatty acid complexes prepared with different amylose chain lengths

M.C. Godet, H. Bizot & A. Buléon*

I.N.R.A., BP 1627, 44316 Nantes cedex, France

(Received 1 September 1994; revised version received 30 December 1994; accepted 9 January 1995)

Highly crystalline samples were prepared by complexation of five amylose fractions (number average degrees of polymerization (DP) 20, 30, 40, 80 and 900) with three fatty acids. Crystallization was performed in water–DMSO mixture at 90°C. The yields of crystallization increased with increasing amylose chain lengths. Moreover, DP20 amylose never precipitated whatever fatty acid was used. All complexes presented similar diffraction diagrams characteristic of the V_h amylose complex structure with narrow peaks. Broader diffraction bands for the DP30–C16 complex indicated smaller crystal domains in the latter case. The melting temperatures of these different complexes increased with amylose chain length; this result suggests a crystallite size dependence on amylose chain length.

INTRODUCTION

Starch is composed of two main components: amylose, a mainly linear polymer of about 500–6000 α-D glucosyl residues and amylopectin, a highly branched polymer of α-D glucosyl distributed in 15–60 residues per chain. It is well known that amylose can form complexes with molecules such as iodine, alcohols and lipids whereas amylopectin forms these complexes only weakly or not at all (Morrison *et al.*, 1993; Sarko & Zugenmaier, 1980). The biosynthesis *in situ* of amylose–lipid complexes in starch, with naturally occurring fatty acids and phospholipids, has been demonstrated (Morrison, 1993; Morrison *et al.*, 1993); but their crystalline nature is still debated (Biliaderis, 1992; Gernat *et al.*, 1993; Morrison, 1993), such structures would be of limited extent and insufficiently perfect to be detected by X-ray diffraction in native starch. Many authors showed that complex formation occurs during heat/moisture treatments, especially during gelatinization of starches naturally containing lipids (Kugimiya *et al.*, 1980; Kugimiya & Donovan, 1981) or when lipids are added to defatted starches (Biliaderis *et al.*, 1986*a*) or pure amylose free of natural lipids (Biliaderis *et al.*, 1985). Both naturally occurring and heat formed complexes show specific properties such as a decrease in amylose solubility or an increase in gelatinization temperatures (Eliasson *et al.*, 1981; Morrison, 1993). Polar lipids, e.g. fatty acids and their monoglyceride esters are of technological importance in starch systems causing a reduction in stickiness, improved freeze–thaw stability (Mercier *et al.*, 1980) and retardation of retrogradation. The most important example is probably the use of fatty acids and monoglycerides as anti-staling agents in bread and biscuits: incorporation of such additives in the dough induces a slower crystallization (retrogradation) of the amylopectin fraction and, therefore, retards the staling of bread (Krog, 1971). Moreover, recent studies have demonstrated that a fraction of starch called 'resistant starch' containing essentially gelatinized starch and complexed starch escapes digestion (Englyst *et al.*, 1987; Siljestrom *et al.*, 1989).

Up to now, many studies have dealt exclusively with the influence of the nature of lipids on the complexation with amylose. This article focuses on the influence of amylose chain length (degree of polymerization) on the crystallization and the thermal stability of amylose/fatty acid complexes obtained from different combinations of amylose fractions and fatty acids.

EXPERIMENTAL

Materials

Amyloses and fatty acids

Five fractions of amyloses, later on defined by their DP_n were used. DP20 and DP30 were respectively prepared by mild acid hydrolysis of potato and wrinkled pea starches as described by Robin *et al.* (1974). DP40 was obtained by enzymatic hydrolysis of pea amylose gel

*To whom correspondence should be addressed.

(6% w/w) (Leloup *et al.*, 1991). DP80 and DP900 were respectively purchased from Hayashibara Biochemical Laboratories (Japan) and Avebe (Netherlands) and used without further purification. Caprylic (C8), lauric (C12) and palmitic (C16) acids were supplied by Aldrich-Chemie (Germany).

Molecular weight determination

The number-average molecular weight of DP20, 30 and 40 was studied using size-exclusion chromatography (SEC) on a Superose 12TM column (Pharmacia) in 0·1 M KOH. The column was calibrated as described previously (Leloup *et al.*, 1992). The number-average molecular weight of DP80 and 900 were determined by a combination of high performance size exclusion chromatography (HPSEC) and multi-angle laser light scattering (MALLS) detection (Dawn-F from Wyatt Technology Corporation-Santa Barbara, CA, USA), as previously described by Roger & Colonna (1993). In that case, polydispersity was found to be 1·8 for both samples.

Crystallization of amylose–fatty acid complexes

Crystallization of amylose–fatty acid complexes was performed in water–DMSO mixture (Eliasson & Krog, 1985; Biliaderis *et al.*, 1985). Amylose dispersions (60 mg/ml, 10 ml) and fatty acid solutions in Me_2SO were mixed at 90°C (weight ratio of amylose to added ligand: 10/1) and 25 ml of water were subsequently added. Then, the mixture was cooled to 25°C at a rate of 5°C/h. The precipitated complexes were recovered by centrifugation, washed four times in a 50/50 (v/v) ethanol/water mixture and then stored above a saturated salt solution generating an equilibrium relative humidity of 75%.

The yield (Y) of highly crystalline solid complex precipitation was expressed as the ratio of the number of moles of complexed amylose recovered to the total initial number of moles in percent. This required the determination of the composition of the complexes. The carbohydrate content from the known dry basis was determined following the sulphuric/orcinol derivatization method (Tollier & Robin, 1979).

X-ray diffraction

X-ray diffraction diagrams were recorded using an Inel X-ray equipment operating at 40 kV and 30 mA. $CuK\alpha_1$ radiation (0·15405 nm) was selected using a quartz monochromator. A 120°C (2Θ) curve position sensitive detector (CPS 120, Inel, France) was used to monitor the diffracted intensities over a 2 h exposure period. The samples (100 mg dry matter) were sealed between two aluminium foils to prevent any significant water exchange during the measurements.

Determination of crystallinity

The apparent crystallinity ratio of amylose–fatty acid complexes was calculated according to Murthy and Minor's method (1990). The diffraction patterns were normalized to the total diffused intensity between 3 and 30° (2Θ). The background level and the diffusion due to the amorphous fraction were estimated in the same range. The diffusion due to the amorphous fraction was approximated with a third degree polynomial fitted to the main minima, yielding a diffusion component very similar to experimental diagrams obtained with amorphous starches.

Crystallinity (X_c) was calculated between 3 and 30° (2Θ) as follows:

$$X_c = \frac{(S_{total}\text{-}S_{bck})\text{-}(S_{amorphous}\text{-}S_{bck})}{S_{total}\text{-}S_{bck}}$$

with: S_{total}, integrated intensity of sample; $S_{amorphous}$, integrated intensity corresponding to the fitted amorphous fraction; S_{bck}, integrated intensity of the background.

Differential scanning calorimetry

The DSC thermograms were obtained with a Setaram DSC111 equipment. Temperature and enthalpy conditions were checked with indium ($T_m = 429{\cdot}8$ K, $\Delta H_m = 28{\cdot}55$ J/g). Samples (about 20 mg) were prepared and weighed in stainless steel pans. Approximately 85 μl of distilled water were added to reach water contents around 75% before sealing. The DSC scan was performed from 30 to 150°C at a scanning rate of 3°C/min, the reference pan contained 110 μl of water. Following heat treatment, the dry matter of the complexes was precisely determined in the open cut pans by oven drying for 3 h at 130°C (accuracy: ±0·5% H_2O dry basis).

The transition enthalpies (ΔH) were calculated from the peak area using a linear baseline and expressed as joules per gram of dry complex. Reproducibility of maximum peak temperature was typically ±0·5°C and enthalpies were reproducible within 3% for sharp peaks and 6% for extended transitions due to difficulties in choosing onset and end temperatures. Most measurements were done in triplicate.

RESULTS

Crystallization

The precipitation/crystallization temperature appeared optimal at 90°C. Both crystallinities and enthalpies were maximized and solvent boiling was avoided under atmospheric pressure. Yields of crystallization (Y%) are presented in Table 1. They comprised between 42% for

Table 1. Yields of complexed amylose vs DP of amylose and fatty acid aliphatic chain length, the yield is expressed as the number of moles of complexed amylose divided by the initial number of moles used for crystallization (%)

	DP30	DP40	DP80	DP900
C8	565·1	62·3	85·6	95·9
C12	44·5	67·0	90·6	97·2
C16	42·0	62·0	86·1	96·6

the DP30–C16 complex and 97% for the DP900–C16 or C12 complex. Complexation with the DP20 amylose never yielded significant amount of precipitate to be used for further experiments whatever the fatty acid. With other amylose fractions, the complexation yield increased with the DP and remained below 60% for DP30. *Y* appears to be more sensitive to amylose molecular weight (chain end effects) than the number of carbons of the fatty acids.

For all amylose fractions, control samples free of fatty acid produced crystalline precipitates characteristic of the B-type amylose. DP20 amylose remained the exception and never precipitated under our conditions.

X-ray diffraction

For all complexes obtained, X-ray diffraction diagrams were typical of the V_h form of amylose (Rappenecker & Zugenmaier, 1981) with the three main reflections corresponding to the Bragg angles $2\Theta = 7{\cdot}4°$, $12{\cdot}9°$, $19{\cdot}8°$ (Fig. 1). Minor reflections at $2\Theta = 10{\cdot}0°$, $17{\cdot}0°$, $18{\cdot}0°$ and $22{\cdot}5°$ were also observed. The sharpness of the peaks was high and the amorphous diffusion rather weak for this type of substrate, except for the DP30–C16 complex which showed broad diffraction peaks and a conspicuous diffusion pattern. The relative intensities were similar for C12 and C16 complexes, the most intense reflection being observed at 19·8° and 12·9° for C8 complexes.

Crystallinities were also very similar for all complexes (Table 2) ranging from 45 to 59%; the complexes obtained with longer C12 and C16 fatty acids lying at the high end but DP30–C16 complex being the exception.

Differential scanning calorimetry

Thermograms are presented in Fig. 2, melting temperatures (T_m taken at peak maximum) and enthalpies are given in Table 3. A low temperature transition was always observed for the complexes produced with the palmitic acid. It was attributed to the uncomplexed fatty acid material ($T_m = 62°C$). Based on their enthalpies of fusion, the fraction of residual lipid was calculated. This lipid represented only 1·6% compared to the initial fatty acid for the DP30–C16 complex, 0·3% for the DP40–

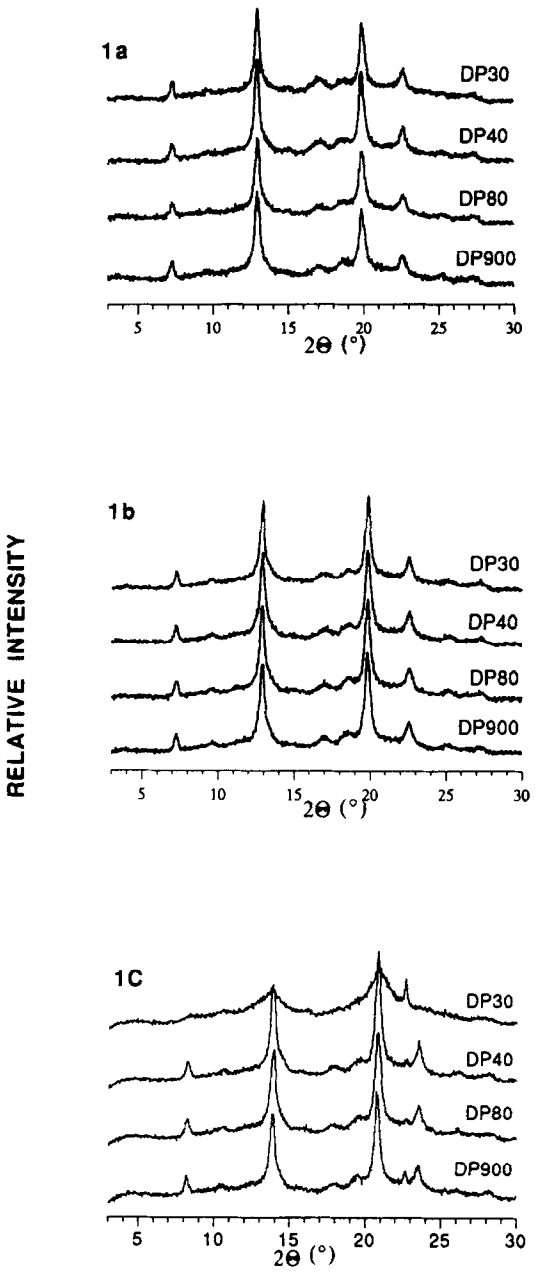

Fig. 1. V-type X-ray diffractograms of amylose/fatty acid complexes – complexing fatty acids: (a) caprylic C8; (b) lauric C12; (c) palmitic C16.

Table 2. Crystallinity of the amylose–fatty acid complexes (%)

	DP30	DP40	DP80	DP900
C8	45	45	49	50
C12	55	59	59	57
C16	45	58	59	53

C16 complex, 0·2% for the DP80–C16 complex and 0·1% for the DP900–C16 complex. Moreover, thermograms of amylose–palmitic acid complexes obtained after washing with a non-polar solvent (ether), no longer presented this endotherm characteristic from

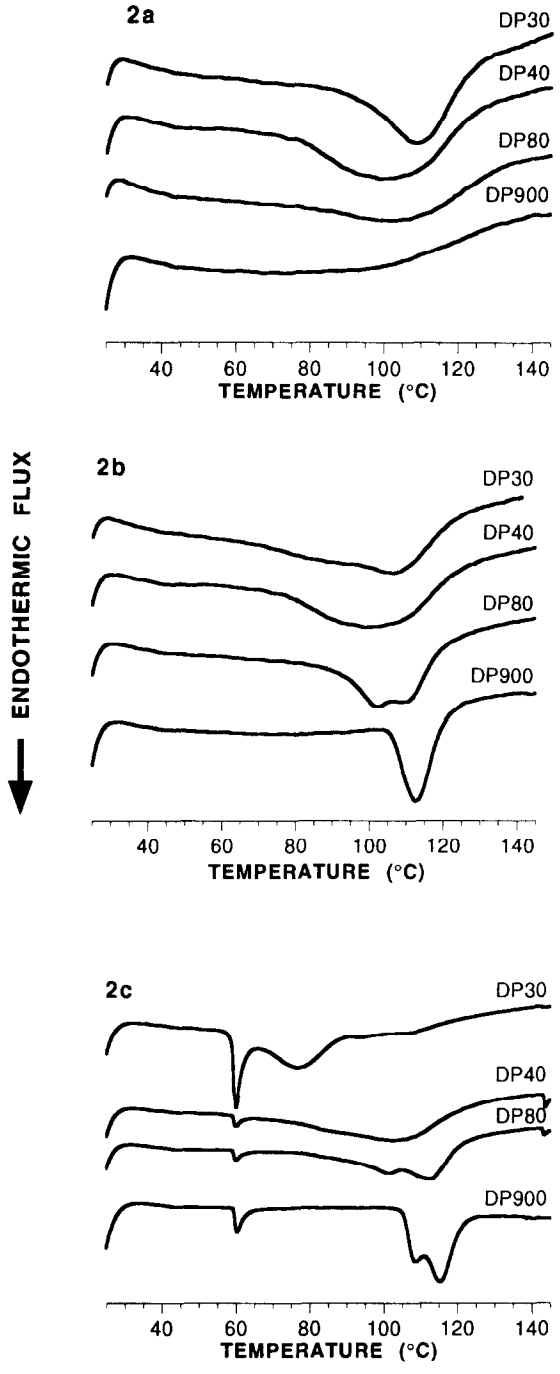

Fig. 2. D.S.C. traces of amylose/fatty acid complexes – complexing fatty acids: (a) caprylic C8; (b) lauric C12; (c) palmitic C16.

residual fatty acid in agreement with uncomplexed lipid extraction procedures (Morrison, 1981).

Melting of most complexes occurred as a main wide transition, a low temperature shoulder appeared and seemed to be clearly identified for DP30–C16 (78·5°C), DP80–C16 (102°C), DP900–C16 (109°C) and DP80–C12 (102°C). The endotherms were very broad although the sharpness of diffraction patterns, especially for low molecular weight amylose fractions or C8 fatty acid would suggest that clear cut transitions should appear.

Table 3. Maximum peak temperatures (°C) with occasional shoulder (in italics) and enthalpies of endotherms in J/g dry complex (quoted between brackets) of the amylose–fatty acid complexes (nd: not determined)

	DP30		DP40		DP80		DP900	
C8		109		102		107		nd
		(30·4)		(27·0)		(20·8)		(nd)
C12	*87*	106		102	*102*	110		113
		(25·5)		(28·0)		(26·3)		(16·3)
C16	*78*	109		105	*102*	113	*109*	115
	(*10·3*)	(2·9)		(33·3)		(28·1)		(24·6)

For DP900–C8 no distinct endotherm was observed but for a slight curvature in thermograms. The melting temperatures of the different complexes was in the range 78–115°C and generally increased with the amylose chain length.

The melting enthalpies, ranged from 16·3 to 33·3 J/g dry matter. The general trend was a slight increase with increasing fatty acid chain length, and a decrease with increasing amylose DP except for DP30.

DISCUSSION

A single crystallization procedure has been chosen for all combinations of amylose fractions and fatty acids in order to compare the effect of amylose chain length on the characteristics of the complexes. The DMSO–water system was selected to eliminate the influence of amylose chain lengths on solubility in the organic solvent and to take advantage of water as a precipitant.

The increase in crystallization yields with amylose chain length could be explained by a combination of amylose solubility and the ability to form the complexes and precipitate in the crystallization medium. In this respect our conditions are likely not to be the most suitable ones for low DP amylose (DP15 and DP30) since water remains a fairly good solvent at the precipitation temperature. Conversely metastable solutions of low DP obtained after dialysis may be used to prepare lamellar crystals (Buléon *et al.*, 1983; Brisson *et al.*, 1991). Complexation with lower DP seems to be hampered by reversible solubility and the critical size seems to be around 30–40 glucosyl residues to complex palmitic acid and 20–30 glucosyl residues for lauric and caprylic acids, i.e. about the chain length to accommodate two fatty acids per chain. This provides an extra argument to understand why amylopectin with short side chains (DP 15–20) (Robin *et al.*, 1974) cannot form any inclusion compounds, other reasons may be related to single helical conformation, branching flexibility and intramolecular crowding.

For all complexes studied here the calculated crystallinities were very similar, except for a slightly lower level with caprylic acid and DP30–C16 complex. However, the values obtained may not reflect the crystalline size

effects causing peak broadening as for DP30–C16 complex which most likely contains smaller crystallites. When precipitation temperatures lower than 90°C were tested, the complexes were less crystalline as evidenced by X-ray diffraction, and the melting traces observed by DSC involved multiple endotherms at lower temperatures. This may be connected to some structural reorganizations induced by temperature during heating. The optimum temperature for V_h complex formation has also been determined to be 90°C when casting corn starch films (Bader & Göritz, 1994). On average this temperature is close to the T_{onset} of endotherms or about T_{max}-20/30°. Our complexation procedure aimed at promoting the crystallization of 'form II' complexes as denoted by Biliaderis *et al.* (1985) for amylose–monoglycerides complexes. This crystalline form would consist of polycrystalline aggregates, giving the typical reflections of the V_h-type amylose, while 'form I' consists of unpacked helical amylose chain segments and presents amorphous X-ray diagrams and low-temperature melting endotherms. The 'form I' is obtained at lower temperatures (60°C) by favouring rapid nucleation. This effect of the crystallization temperature on the crystallinity of complexes has also been reported for amyloses and monoglycerides (C_{10}–C_{18}, Biliaderis *et al.*, 1985; Galloway *et al.*, 1989; Seneviratne & Biliaderis, 1991), lauric acid (Biliaderis *et al.*, 1986*b*) or alcohols (Kowblansky, 1985; Whittam *et al.*, 1989).

Melting temperatures of amylose–fatty acid complexes increased with the length of the fatty acid for DP40, DP80 and DP900, and with the amylose chain length for complexes prepared with C12 and C16 fatty acids. Such an evolution with the lipid chain length has already been reported by several authors on amylose–monoglyceride complexes (Stute & Konieczny-Janda, 1983; Eliasson & Krog, 1985; Biliaderis *et al.*, 1985; Karkalas & Raphaelides, 1986). The observed evolution of melting temperatures with the DP should be related to improved crystalline features and especially crystallite size. This is not obvious on X-ray diffraction diagrams (Fig. 1) except with DP30–C16 complexes for which wider diffraction peaks and the low temperature (78·5°C) endotherm observed in thermograms may agree with smaller crystallites. Nevertheless, if the crystallite size increase occurs along the macromolecular chain axis, it may not be visible on the width of major diffraction lines observed, since they correspond to crystallographic planes (110), (130), (310) and (330) (Rappenecker & Zugenmaier, 1981).

The bimodal melting behaviour of complexes prepared with C12 and C16 fatty acids may exemplify annealing and/or recrystallization effects which should be checked by X-ray diffraction/thermal analysis coupling and kinetic D.S.C. studies. Thus DSC patterns observed here result from a combination of annealing and melting kinetics of various complexes precipitated and crystallized at temperatures variably distant from their intrinsic melting temperatures of well tempered crystalline phases. Further investigations combining various kinetics may clarify our partial data as exemplified by Biliaderis and Seneviratne (1990) who identified forms IIa and IIb. In any case, the extended endotherms displayed with caprylic acid (C8) remain difficult to interpret. They are unlikely to be due to large amounts of defects in crystals or very small crystal sizes when considering the sharpness and intensity of the diffraction lines.

In contrast and still in agreement with Biliaderis and Seneviratne (1990) only minor evolutions of enthalpies have been observed. Since non-crystalline form I and crystalline form II complexes develop very close total endothermic effects upon heating, the interchain packing energy has been considered to be almost negligible compared to the total enthalpy of dissociation, solvation and uncoiling. Separate analysis of the different contributions is difficult to conduct due to the overlapping of concurrent phenomena.

CONCLUSION

Crystallization conditions have been optimized to produce satisfactory V_h-type amylose-lipid complexes. Crystallization yield increases with amylose chain length and higher DP favour higher-melting complexes. However metastable structures may be present in the precipitates as suggested by the multimodal or extended D.S.C. traces. Further studies will concentrate on stoechiometric and structural arguments to clarify the mechanism of fatty acids complexation.

REFERENCES

Bader, H.B. & Göritz, D. (1994). Investigations on high amylose corn starch films — 1. Wide angle X-ray scattering (WAXS). *Stärke*, **46**, 229–32.

Biliaderis, C.G. (1992). Structures and phase transitions of starch in food systems. *Food Technol.*, **6**, 98–109.

Biliaderis, C.G., Page, C.M. & Maurice, T.J. (1986*a*). On the multiple melting transitions of starch/monoglycerides systems. *Food Chem.*, **22**, 279–95.

Biliaderis, C.G., Page, C.M. & Maurice, T.J. (1986*b*). Non equilibrium melting of amylose-V complexes. *Carbohydr. Polym.*, **6**, 269–88.

Biliaderis, C.G., Page, C.M., Slade, L. & Sirett, R.R. (1985). Thermal behavior of amylose–lipid complexes. *Carbohydr. Polym.*, **5**, 367–89.

Biliaderis, C.G. & Seneviratne, H.D. (1990). On the supermolecular structure and metastability of glycerol monostearate–amylose complex. *Carbohydr. Polym.*, **13**, 185–206.

Brisson, J., Chanzy, H. & Winter, W.T. (1991). The crystal and molecular structure of V_h amylose by electron diffraction analysis. *Int. J. Biol. Macromol.*, **31**, 31–9.

Buleon, A., Duprat, F., Booy, F.P. & Chanzy, H. (1984). Single crystals of amylose with a low degree of polymerisation. *Carbohydr. Polym.*, **4**, 161–73.

Eliasson, A.C., Carlson, T.L., Larsson, K. & Miezis, Y. (1981). Some effects of starch lipids on the thermal and rheological properties of wheat starch. *Stärke*, **33,** 130.

Eliasson, A.C. & Krog, N. (1985). Physical properties of amylose–monoglyceride complexes. *J. Cereal Sci.*, **3,** 239–48.

Englyst, H.L., Trowell, H., Southgate, D.A. & Cummings, J.H. (1987). Dietary fibre and resistant starch. *Am. J. Clin. Nutr.*, **46,** 873–4.

Galloway, G.I., Biliaderis, C.G. & Stanley, D.W. (1989). Properties and structure of amylose–glycerol monostearate complexes formed in solution or on extrusion of wheat flour. *J. Food Sci.*, **54,** 950–57.

Gernat, C., Radosta, S., Anger, H. & Damashun, G. (1993). Crystalline parts of three different conformations detected in native and enzymatically degraded starches. *Stärke*, **45**(9), 309.

Karkalas, J. & Raphaelides, S. (1986). Quantitative aspects of amylose–lipid interactions. *Carbohydr. Res.*, **157,** 215–34.

Kowblansky, M. (1985). Calorimetric investigation of inclusion complexes of amylose with long-chain aliphatic compounds containing different functional groups. *Macromolecules*, **18,** 1776–9.

Krog, N. (1971). Amylose complexing effect of food grade. *Stärke*, **22,** 206–10.

Kugimiya, M. & Donovan, J.W. (1981). Calorimetric determination of the amylose content of starches based on formation and melting of the amylose–lysolecithin complex. *J. Food Sci.*, **46,** 765–77.

Kugimiya, M., Donovan, J.W and Wong, R.Y. (1980). Phase transitions of amylose–lipid complexes in starches: a calorimetric study. *Stärke*, **32,** 265–70.

Leloup, V., Colonna, P. & Buléon, A. (1991). Influence of amylose–amylopectin ration on gel properties. *J. Cereal Sci.*, **13,** 1.

Mercier, C., Charbonniere, N., Grebaut, J. & de la Gueriviere, J.F. (1980). Formation of amylose complexes by twin-screw extrusion cooking of manioc starch. *Cereal Chem.*, **57,** 4–9.

Morrison, W.R. (1981). Starch lipids: a reappraisal. *Stärke*, **33,** 408–10.

Morrison, W.R. (1993). In *Seed Storage Compounds: Biosynthesis, Interactions and Manipulation*, P.R. Shewry & K. Stobart, Eds. Oxford University Press, Oxford, pp. 175–90.

Morrison, W.R., Tester, R.F., Snape, C.E., Law, R. & Gidley, M.J. (1993). Swelling and gelatinization of cereal starches. IV. Some effects of lipid-complexed amylose and free amylose in waxy and normal barley starches. *Cereal Chem.*, **70,** 385–91.

Murthy N.S. & Minor H. (1990). General procedure for evaluating amorphous scattering and crystallinity from X-ray diffraction scans of semicrystalline polymers. *Polymer*, **31,** 996–1002.

Rappenecker, G. & Zugenmaier, P. (1981). Detailed refinement of the crystal structure of V_h amylose. *Carbohydr. Res.*, **89,** 182–8.

Robin, J.P., Mercier, C., Charboniere, R. & Guilbot, A. (1974). Lintnerized starches. Gel filtration and enzymatic studies of insoluble residues from prolonged acid treatment of potato starch. *Cereal Chem.*, **51,** 389–406.

Roger, P. & Colonna, P. (1993). Evidence of the presence of large aggregates contaminating amylose solutions. *Carbohydr. Polym.*, **21,** 83–9.

Sarko, A. & Zugenmaier, P. (1980). In *Fiber Diffraction Methods*, A.D. French & K.C. Gardner, Eds. ACS Symposium Series, **141,** 459–82.

Seneviratne, H.D. & Biliaderis, C.G. (1991). Action of α-amylases on V-amylose superstructures. *J. Cereal Sci.*, **131,** 129–43.

Siljestrom, M., Eliasson, A.C. & Bjorck, I. (1989). Characterization of resistant starch from autoclaved wheat starch. *Stärke*, **41,** 147–51.

Stute, R. & Konieczny-Janda, G. (1983). DSC-Unterscuchungen an Stärken. Teil II. Untersuchungen an Stärke-Lipid-Komplexen. *Stärke*, **35,** 340–47.

Tollier, M. & Robin, J. (1979). Adaptation de la méthode à l'orcinol sulfurique au dosage automatique des glucides neutres totaux, conditions d'applications aux extraits d'origine végétale. *Ann. Technol. Agric.*, **28,** 1–15.

Whittam, M.A., Orford, P.D., Ring, S.G., Clark, S.A., Parker, M.L., Cairns, P. & Miles, M.J. (1989). Aqueous dissolution of crystalline and amorphous amylose–alcohol complexes. *Int. J. Biol. Macromol.*, **11,** 339–44.